Erzincan Üniversitesi
Fen Bilimleri Enstitüsü Dergisi
2025,18(1), 59-72
ISSN: 1307-9085, e-ISSN: 2149-4584
Araştırma Makalesi

Erzincan University
Journal of Science and Technology
2025,18(1), 59-72
DOI: 10.18185/erzifbed.1437504
Research Article

Quercetin/Fe_3O_4@Cu(II) Hybrid Structures Fabrication and Cytotoxic Activity

Burcu SOMTURK YILMAZ[1*]

[1]Drug Application and Research Center, Erciyes University, 38280 Kayseri, Türkiye

Received: 15/02/2024, **Revised:** 07/10/2024, **Accepted:** 07/11/2024, **Published:** 28/03/2025

Abstract

In this study, firstly, the synthesis of magnetic iron (Fe) materials (Fe_3O_4 Ms) was carried out and then quercetin was immobilized into the synthesized nanomaterial. Synthesis of organic@inorganic hybrid nanoflowers (Quercetin/Fe_3O_4@Cu(II) hNFs) was carried out using quercetin as the organic component and Cu (II) metal ions and Fe_3O_4 as inorganic components. Characterization of Quercetin/Fe_3O_4@Cu (II)hNFs was carried out using various methods such as FTIR, XRD, SEM, EDX, NTA, and elemental mapping. Then, the cytotoxic activities of Quercetin/Fe_3O_4@Cu(II) hNFs were evaluated by the MTT method using the MCF7 (breast cancer) cell line.

Keywords: Nanoflower; Fe_3O_4, Quercetin

Kuersetin/Fe_3O_4@Cu(II) Hibrit Yapıların Üretimi ve Sitotoksik Aktivite

Öz

Bu çalışmada öncelikle manyetik demir malzemelerinin sentezi gerçekleştirildi ve daha sonra sentezlenen materyal içerisine quercetin immobilize edildi. Organik@inorganik hibrit nanoçiçeklerin (Kuersetin/Fe_3O_4@Cu(II)hNF'ler) sentezi, organik bileşen olarak kuersetin ve inorganik bileşenler olarak Cu(II) metal iyonları ve Fe_3O_4 kullanılarak gerçekleştirildi. Kuersetin/Fe_3O_4@Cu(II)hNF'lerin karakterizasyonu FTIR, XRD, SEM, EDX, NTA ve elemental haritalama gibi çeşitli yöntemler kullanılarak gerçekleştirildi. Daha sonra Kuersetin/Fe_3O_4@Cu(II) hNF'lerin sitotoksik aktiviteleri MCF7 (meme kanseri) hücre hattı kullanılarak MTT yöntemiyle değerlendirildi.

Anahtar Kelimeler: Nanoçiçek, Fe_3O_4, Kuersetin

*Corresponding Author: burcu_smtrk@hotmail.com
Burcu SOMTÜRK, https://orcid.org/ 0000-0002-2775-3083

1. Introduction

Nowadays, loading the active ingredients of drugs into nano-drug delivery systems to increase their effects, reduce their side effects, and ensure their targeted and controlled release is one of the hottest and most current topics in pharmaceutical research. In this direction, hundreds of natural and/or polymeric nano-drug delivery systems are used [1-3]. Nano-drug delivery systems provide high effects in small doses as they deliver therapeutic molecules directly to the cancer tumor site [4]. In addition, the water solubility of the active molecules entrapped in the nano drug delivery system increases and, most importantly, they gain stability. In recent years, studies on the use of copper together with antioxidant compounds in cancer treatment have increased [5-7]. Today, it is used in cancer treatment by taking advantage of the pro-oxidant effects of polyphenolic compounds.

It has applications in medicine, especially as anticancer, anti-inflammatory [8], and antiparasitic drugs, as a carrier system for proteins, and also in the production of improved biocompatible materials [9-10]. There are many advantages to using nano-sized particles. These can be listed as follows. Nanoparticles have small particle sizes, allowing them to pass through small capillaries and be taken into the cell. As the surface area increases, their solubility also increases, and as a result of the increase in solubility, it has many advantages such as increasing the absorption of the particle and therefore its bioavailability.

Quercetin is a flavonoid found in apples, tomatoes, blueberries, and many plants [11]. Although quercetin is known to have antioxidant, anti-inflammatory, antiplatelet, and vasodilator effects, the mechanism of action of most of them has not been fully elucidated. Studies focus on strategies to increase the bioavailability of quercetin [12]. Quercetin shows promise as a potential anti-cancer agent. The fact that quercetin has many different biological activities, including antioxidant, anti-inflammatory, antiproliferative, proapoptotic, and antiangiogenic, suggests that it can be considered a natural anti-cancer agent. Due to these properties, it is recommended to be used in combined treatment with other anticancer agents.

For this reason, many material groups or complex compounds are available in the literature [13-17]. Hybrid nanoflowers, which are among these material groups, attract much attention in this field. Hybrid nanoflowers, which are a new member of the nanoparticle and have been preferred in many studies in recent years, have unique properties. It has a very large surface area due to its flower-like structure. It also exhibits very excellent activity and stabilization. Hybrid nanoflowers consist of organic and inorganic parts. The organic part may contain enzymes, proteins, plant extracts, and organic molecules, while the inorganic part contains various metal ions (such as Copper, Zinc, Manganase, and Cobalt).

In this study, new organic-inorganic hybrid nanoflower Quercetin/Fe_3O_4@Cu(II) hNFs were successfully synthesized by a fast and simple method involving many steps. Quercetin/Fe_3O_4@Cu(II) hNFs were characterized by FT-IR, XRD, SEM, EDX, and NTA. Then, the cytotoxic activities of synthesized hNFs and quercetin were evaluated on the MCF7 cell line.

2. Material and Methods

Materials

Iron (III) chloride hexahydrate, Iron (II) chloride heptahydrate, and sodium hydroxide, were purchased from Merck. Quercetin, Copper(II) sulfate pentahydrate, Sodium chloride, potassium chloride, potassium dihydrogen phosphate, sodium hydrogen phosphate, calcium chloride dihydrate, and magnesium chloride hexahydrate were purchased from Sigma-Aldrich.

Synthesis of the Fe_3O_4 nanomaterials

0.64 grams of $FeCl_2.4H_2O$ and 1.64 grams of $FeCl_3.6H_2O$ were taken into 10 mL of pure water and mixed quickly by vortexing. The solution was then stirred in an oil bath at 80°C for 15 minutes and NaOH was added. The mixture was stirred at the same temperature for another 15 minutes and then centrifuged at 10000 rpm for 10 minutes. Then, the pellet part was taken and left to dry in the oven at 50°C [18].

Immobilization method of Quercetin onto iron oxide nanomaterials

Fe_3O_4 nanomaterials-Quercetin were prepared as follows: First of all, 0.5 g of Fe_3O_4 nanomaterials were mixed with 20 mL of methanol, and then 0.05 g of quercetin was added into the mixture. The mixture was then stirred for 6 hours. And finally, the formed particles were dried [19].

Synthesis Quercetin/Fe_3O_4@Cu(II) hybrid nanoflowers

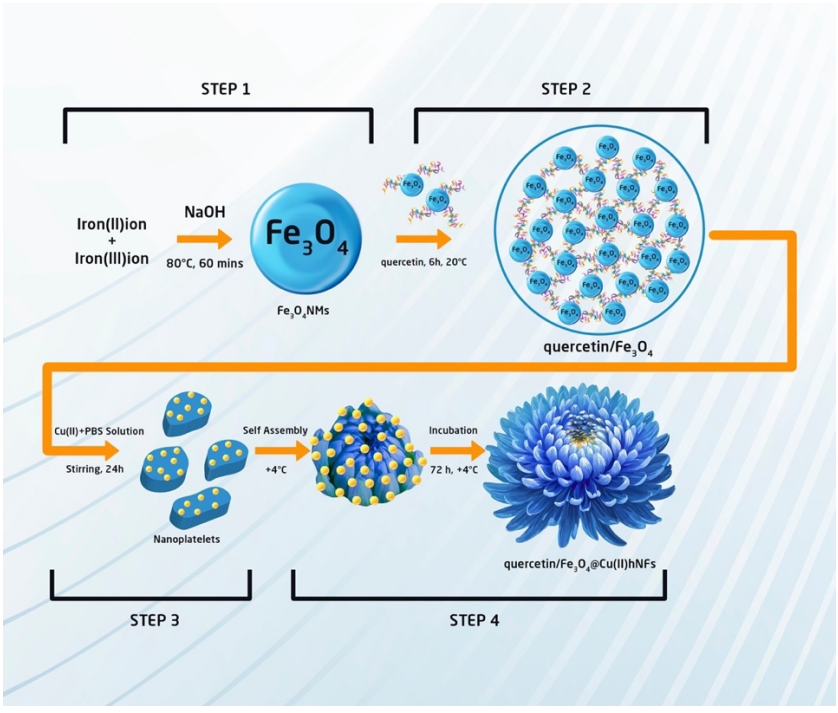

Figure 1. The synthesis scheme of Quercetin/Fe_3O_4@Cu(II) hNFs

Quercetin/Fe_3O_4@Cu(II) hNFs were prepared by subjecting them to some modifications [20-22]. In a 50 mL test tube, 6 mg Quercetin/Fe_3O_4 nanomaterial, PBS buffer (pH:7.4), and 0.003 mL $CuSO_4$ solution (120 mM) were added. The mixtures were stirred for 24 hours and kept at +4 ºC for three days. Then, centrifugation was performed at 10000 rpm for 10 minutes. The resulting precipitates were dried in an oven at ambient temperature. The synthesis scheme of Quercetin/Fe_3O_4@Cu(II) hNFs is shown in Figure 1.

Characterization of Quercetin/Fe_3O_4@Cu(II) hNFs

The morphologies of the hNFs were determined using the SEM device (FESEM, Zeiss GeminiSEM 500). While the presence of elements such as Cu and Fe in the structure of hNFs was determined by EDX (Zeiss, Gemini 500), the distribution of the elements was clarified by elemental mapping. In addition, while the crystal structures were examined using XRD (Panalytical, Empyrean), the presence of oxygen groups bound to phosphorus in the structure was determined by the FTIR (Perkin Elmer, 400 FT-IR/FT-FIR Spectrometer Spotlight 400 Imaging System) spectrum. Dimensional analysis was determined using the NTA (Malvern Panalytical, Nanosight NS300) device.

Cytotoxicity assessment (MTT assay)

The MCF7 cell line was used for the cytotoxic effects of Quercetin/Fe_3O_4@Cu(II) hNFs. For this purpose, screening was performed at concentrations ranging from 7-81 to 500 µg/mL. First, the cancer cell was incubated for 24 hours after being planted on the plate. Then, hNFs and Quercetin were added to the medium at the indicated concentrations, and after staining with MTT dye, an absorbance reading was performed in a microplate reader at 572 nm.

3. Results and Discussion

SEM analysis

The morphologies of the synthesized Quercetin/Fe_3O_4@Cu(II) hNFs were determined by SEM analysis. As seen in Figure 2, it was observed that Quercetin/Fe_3O_4@Cu(II) hNFs had a flower shape.

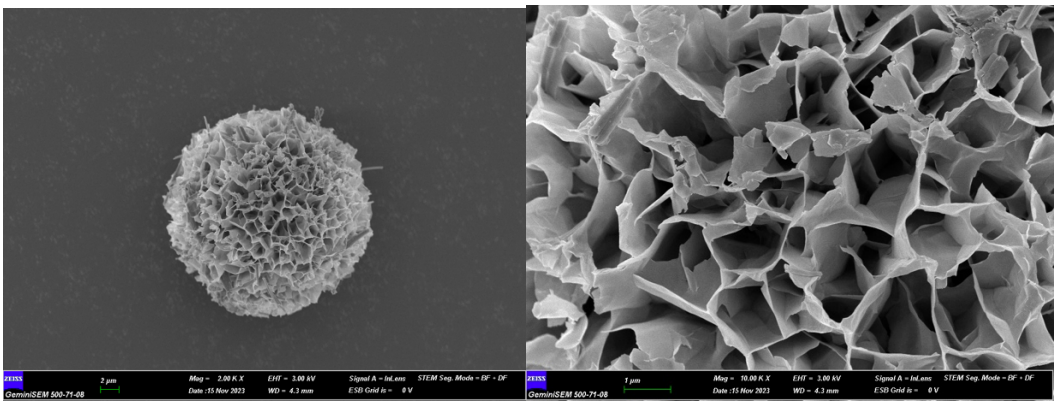

Figure 2. SEM images of Quercetin/Fe_3O_4@Cu(II) hNFs a) 2.00KX, b) 10.000 KX

Noma et al. 2020, synthesized hybrid nanoflowers using L-asparaginase enzyme and Cu metal ion. They observed how their morphology changed at different pH and temperature. They observed that hybrid nanoflowers synthesized using Cu metal ions had a flower-like structure [23]. Somturk et al. (2022) synthesized hybrid nanoflowers using superoxide dismutase enzyme and Cu, Co, Zn, and Mn metal ions. The catalytic activities of the synthesized hybrid nanoflowers were investigated. It was determined that the morphology of hybrid nanoflowers changed as the metal ions changed [24]. Çelik et al. reported that dopamine@Cu hNFs which is close to ideal flower morphology were synthesized at a PBS pH value of 7.4 [25].

EDX analysis

The basic composition and elemental analysis of synthesized Quercetin/Fe_3O_4@Cu(II) hNFs was determined using EDX. The EDX spectrum of synthesized Quercetin/Fe_3O_4@Cu(II) hNFs is given in Figure 3. The presence of Cu and Fe was detected in the structure. Other elements seen in the EDX spectrum (Ca, P, Cl, and O) originate from the PBS buffer present in the medium. PBS buffer contains different salt mixtures. These elements are seen in the spectrum due to the salt content.

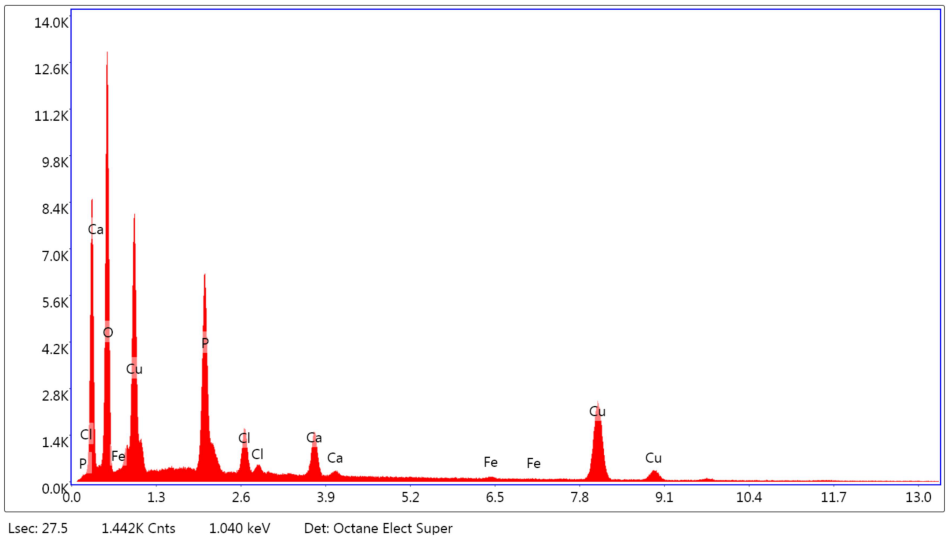

Figure 3. EDX analysis of Quercetin/Fe_3O_4@Cu(II) hNFs

The weight percentage of the O, P, Fe, and Cu elements contained in hNFs were determined at 45.46, 13.24, 4.22, 0.28, and 32.7%, respectively. In addition, the atomic values percentage of hNFs are given as 70.9, 10.67, 0.13, and 12.84 respectively as shown in Table 1.

Table1. Weight and atomic percentage of Quercetin/Fe_3O_4@Cu(II) hNFs

Element	Weight %	Atomic %	Net Int.
O K	45.46	70.9	3033.29
P K	13.24	10.67	1851.05
ClK	3.48	2.45	486.29
CaK	4.85	3.02	563.4
FeK	0.28	0.13	20.83
CuK	32.7	12.84	1382.66

The EDX spectrum used for hybrid nanoflower characterization provides information about the presence and amount of metal ions in the environment. Koca et al. (2024) synthesized hybrid nanoflowers using *Desmarestia menziesii Algae* extract and Cu metal ion. They determined the weight and atomic percentages of metal ions in the synthesized hybrid nanoflowers using the EDX spectrum [26]. Koca et al. (2022) determined the basic skeletal elements (C, O, P, and Cu) of Cu-hNFs synthesized with *Ascoseira mirabilis* extract and determined the weight percentage of Cu to be approximately 15% [27].

Elemental mapping

Base mapping of the synthesized Quercetin/Fe_3O_4@Cu(II) hNFs was performed. As seen in Figure 4, it can be seen that the elements Cu, Fe, O, and P are distributed homogeneously.

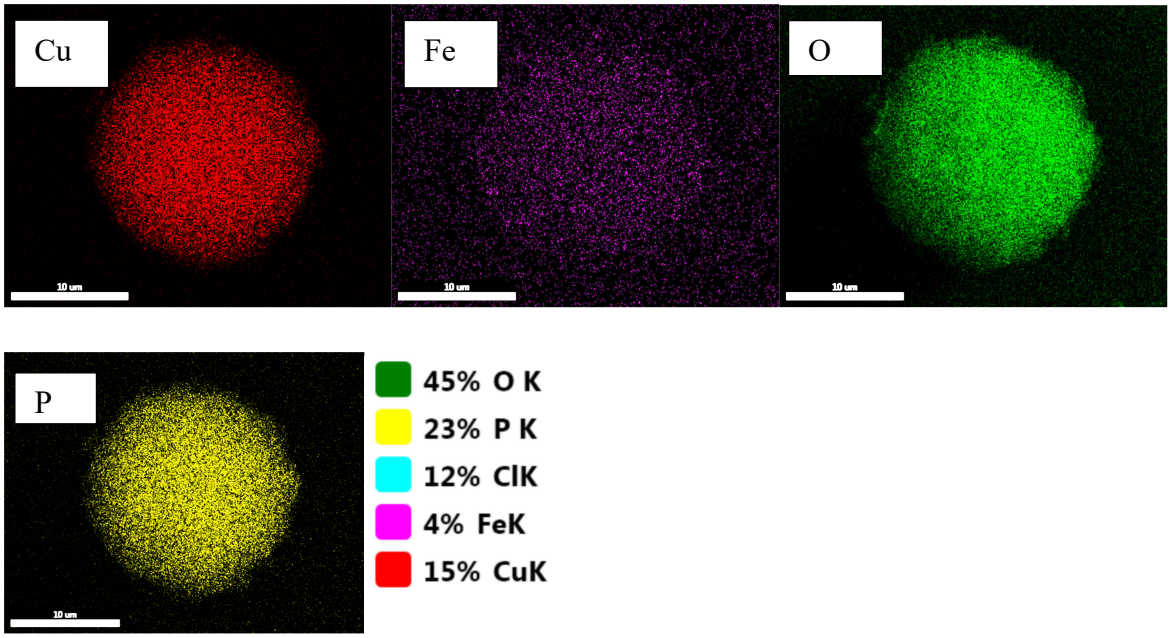

Figure 4. Elemental mapping (Fe, Cu, O, P) of Quercetin/Fe_3O_4@Cu(II) hNFs.

An elemental map is an image that shows the spatial distribution of elements in a sample. Elemental maps are extremely useful for displaying elemental distributions in a textural context, particularly for showing compositional zoning. Somturk et al. (2024) synthesized hybrid nanoflowers using Tribulus Terrestris L. extract and Cu, Co, Zn metal ions. They showed the homogeneous distribution of metal ions by elemental metal mapping of the synthesized hybrid nanoflowers [1]

XRD analysis

The XRD peaks assigned for Quercetin/Fe_3O_4@Cu(II) hNFs are as follows: XRD: 9.10°, 12.96°, 18.79°, 20.87°, 27.38°, 29.48°, 30.64°, 31.74°, 33.71°, 37.21°, 41.59°, 45.48°, 47.74°, 53.46°, 56.48°, 61.10°, 63.57°, 66.22°, 68.19°, 71.42°, 75.26°, 79.06°, 83.95° in Figure 5 compared with JCPDS (00−022−0548) [28]

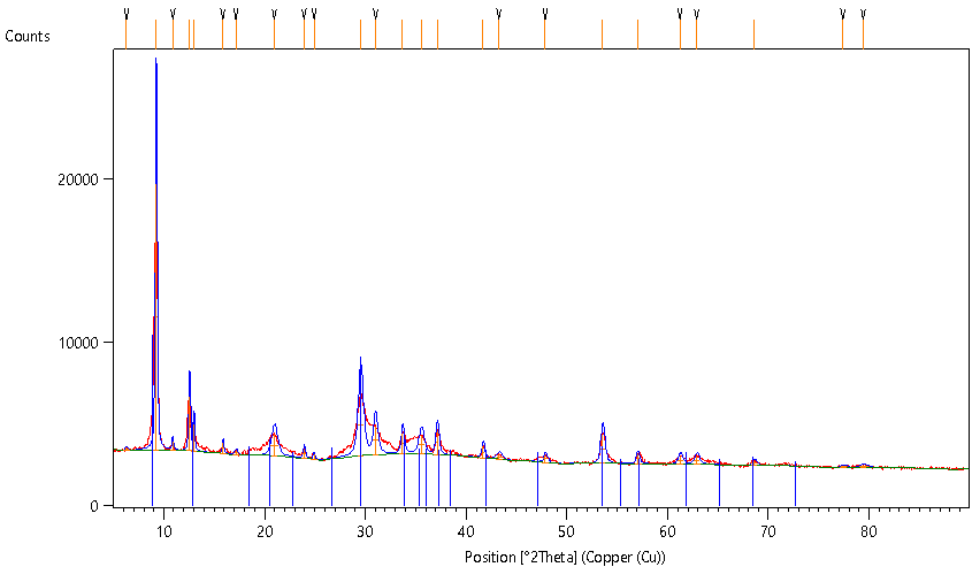

Figure 5. XRD analysis of Quercetin/Fe_3O_4@Cu(II) hNFs

When the synthesized Quercetin/Fe_3O_4@Cu(II) hNFs are compared with the JCPDS (00−022−0548) standard, it is seen that the peaks overlap. In other words, the presence of copper phosphate primary crystals is elucidated.

FTIR analysis

FT-IR (Perkin Elmer Spectrum 400) spectrum was used to observe the characteristic peaks of hNFs. (Fig. 6). For Quercetin/Fe_3O_4@Cu(II) hNFs, the values are as follows; FT-IR (cm^{-1}): 3570 (N–H and O–H stretching), 3324 (Ar–H and C–H stretching), 2907 (C–H, stretching), 2211, 1655, 1172 (P=O), 1083, 1002 (P–O), 647 (O=P=O). Additionally, the iron-bound oxygen (Fe-O) peak is observed at 537 cm^{-1}.

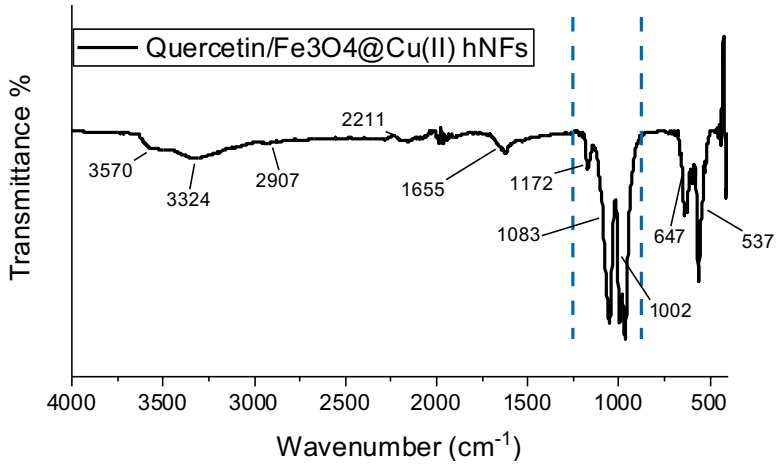

Figure 6. FT-IR spectrum of Quercetin/Fe_3O_4@Cu(II) hNFs

During the synthesis phase of hNFs, first, the Cu metal ion comes together with the phosphate ions in the environment to form copper phosphate crystals. As seen in the FT-IR spectrum, the presence of phosphorus-related oxygen peaks indicates that our crystal structure has been formed. Similar spectra were obtained in previously reported studies [29-32].

NTA Assay

Size analysis of synthesized Quercetin/Fe_3O_4@Cu(II) hNFs was carried out using the NTA device. As seen in Figure 7, the average size of hNFs was 122.1 nm.

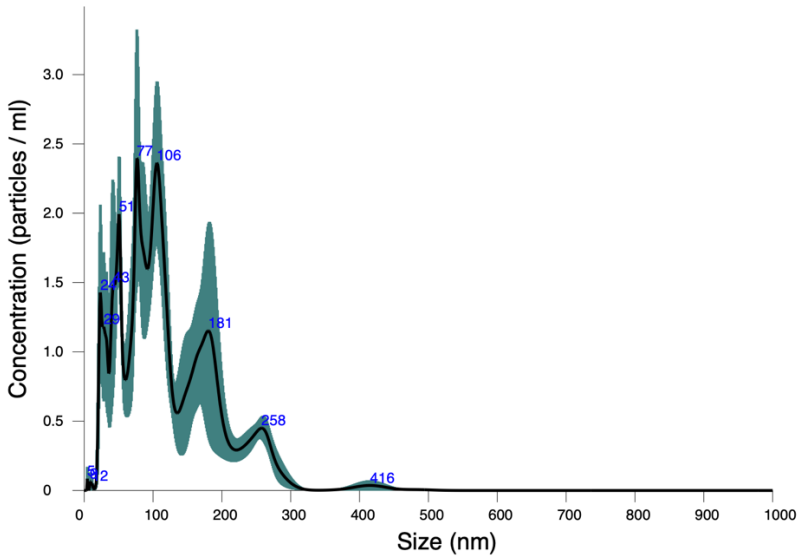

Figure 7. Size analysis of Quercetin/Fe_3O_4@Cu(II) hNFs

Hybrid nanoflowers are formed in both micron and nano sizes. There is no homogeneous distribution in size in the formation of the structures. When looking at the SEM images (Figure 2), it is seen that they are in micron size. However, the NTA device detects particles below 1 micron. This analysis shows the presence of nano-sized particles in the structure.

Cytotoxicity assessment

The effect of Quercetin/Fe_3O_4@Cu(II) hNFs and Quercetin on the viability of MCF7 cell lines is shown in Figure 8.

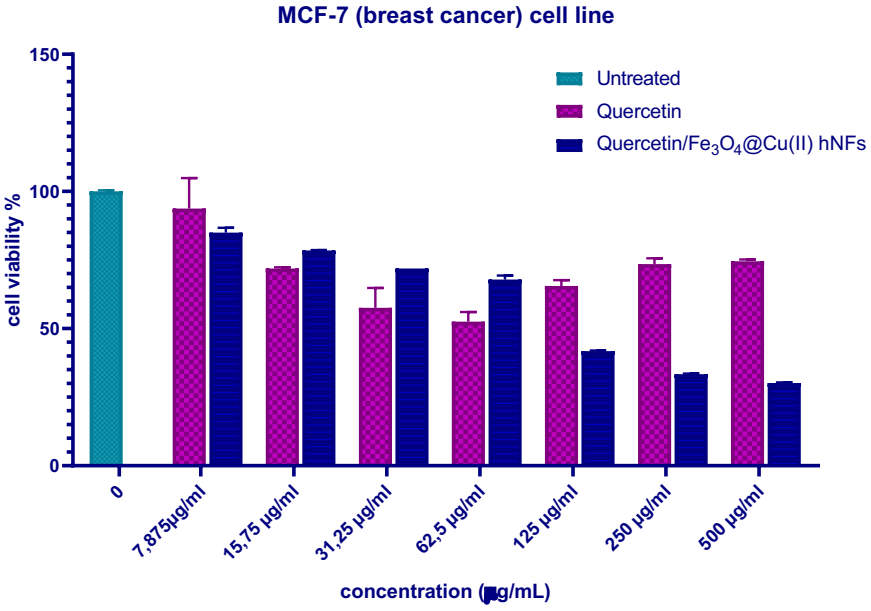

Figure 8. Cytotoxicity of Quercetin and Quercetin/Fe_3O_4@Cu(II) hNFs on MCF7 cell lines, respectively

As seen in Figure 8, the cytotoxic effects of quercetin and Quercetin/Fe_3O_4@Cu(II) hNFs were evaluated on the MCF7 cell line. Although quercetin has a slight effect, similar results were obtained at all concentrations. It caused approximately 40% of cell death. Quercetin/Fe_3O_4@Cu(II) hNFs caused cell death depending on concentration. It caused 75% of cell death. This means that when quercetin was converted into hNFs form, it was observed that its cytotoxic activity increased significantly. As can be seen from the results, it was determined that quercetin had a higher cytotoxic effect when transformed into a hybrid nanoflower form. This situation can be explained as follows: Firstly, since hybrid nanoflowers have a very high surface area due to their morphology, their effectiveness was higher. At the same time, when quercetin was transformed into a hybrid nanoflower form, it turned into a smaller form in size. For this reason, it was easier to take into the cell because the average size of the MCF7 cell line varied between 19.9 and 33.9 µm [33]. Since the synthesized nanoflowers had a smaller morphology, they were easier to take into the cell.

There are many studies on the synthesis and activity of hybrid nanoflowers today. However, there are only a few studies on their cytotoxic activity. Somturk et al. (2024) performed hybrid nanoflower synthesis using *Tribulus Terrestris L.* extract and Cu, Co, and Zn metal ions. They observed that the morphologies of these hybrid nanoflowers differed as the metal ion changed. They also tested their cytotoxic activities on the A549 cell line. As a result, they found that the Co metal ion had better activity than hybrid nanoflowers synthesized with plant extracts and other metal ions [1]. Somturk (2024) synthesized hybrid nanoflowers using gallic acid and Cu, Zn metal ions. They tested their cytotoxic activities on A549 and MCF7 cell lines. Somturk concluded that the cytotoxic activities of hybrid nanoflowers synthesized with Cu metal ions were better than those synthesized with gallic acid and Zn metal ions [34]. Bor et al. synthesized Cu and Zn hybrid nanoflowers using the *Persea americana* Mill. leaves extract. They applied the cytotoxic effects of the metal nanoflowers they synthesized to the L929- mouse fibroblast cell line. They found that the anticancer activity of hybrid nanoflowers synthesized with Cu was higher than that of plant extract. It is concluded that the effectiveness of the plant extract is higher when it is converted into nanoflower form [35].

4. Conclusion

New organic-inorganic hybrid nanoflower (Quercetin/Fe_3O_4@Cu(II) hNFs) were successfully synthesized by a fast and simple method involving many steps. Quercetin/Fe_3O_4@Cu(II) hNFs were characterized by FT-IR, XRD, SEM, EDX, and NTA. Then, the cytotoxic activities of synthesized hNFs and quercetin were evaluated on the MCF7 cell line. When the results were examined, it was observed that when Quercetin was converted into hNFs form, its cytotoxic activity increased significantly. Since hybrid nanoflowers have a larger surface area due to their morphology, they have better interaction and activity capability. Therefore, the hybrid nanoflower synthesized using quercetin can be a therapeutic alternative.

Author Contributions

B.S.Y. performed all experiments. B.S.Y. conceived the original idea and designed the project. B.S.Y. wrote the manuscript.

Acknowledgments

The author would like to thank Erciyes University, Drug Application and Research Center (ERFARMA) for laboratory and device support. We would like to thank the Proofreading & Editing Office of the Dean for Research at Erciyes University for the copyediting and proofreading service for this manuscript

References

[1] Somturk Yilmaz, B., Bekci, H., Altiparmak, A., Uysal, S., Şenkardeş, İ., Zengin, G. 2024. Determination of anticancer activity and biosynthesis of Cu, Zn, and Co hybrid nanoflowers with *Tribulus terrestris* L. extract. Process Biochemistry. 138: 14-22

[2] Uras, I.S, Karslı, B., Konuklugil, B., Ocsoy, I., Demirbas, A. 2023. Organic–Inorganic Nanocomposites of *Aspergillus terreus* Extract and Its Compounds with Antimicrobial Properties. *Sustainability* 2023, *15*(5), 4638; https://doi.org/10.3390/su15054638

[3] Dadi, S., Celik, C., Ocsoy, I., 2020. Gallic acid nanofower immobilized membrane with peroxidase-like activity for m-cresol detection. Gallic acid nanofower immobilized membrane with peroxidase-like activity for m-cresol detection. Scientific Reports. 10:16765

[4]Yoshida, H., Takamura, N., Shuto, T., Ogata, K., Tokunaga, J. ve Kawai, K., 2010, The citrus flavonoids hesperetin and naringenin block the lipolytic actions of TNF-α in mouse adipocytes, Biochemical and Biophysical Research Communications, 394, 728-732.

[5] Zeng, W., Jin, L., Zhang, F., Zhang, C. ve Liang, W., 2018, Naringenin as a potential immunomodulator in therapeutics, Pharmacological Research, 135 (2018), 122–126.

[6]Zhang, J.J., Dong, X., Cao, Y.Y., Yuan, Y. D., Yang, Y.B., Yan, Y.Q., vd., 2020, Clinical characteristics of 140 patients infected with SARS-CoV-2 in Wuhan, China, Allergy, 75, 1730–41. doi: 10.1111/all. 14238.

[7]Zhang, L., Song, L., Zhang, P., Liu, T., Zhou, L., Yang, G., Lin, R. ve Zhang, J., 2015, Solubilities of naringin and naringenin in different solvents and dissociation constants of naringenin, Journal of Chemical & Engineering Data, 60(3), 932-40. https://doi.org/10.1021/je501004g.

[8]Wang, M.J., Chao, P.D., Hou, Y.C. ve Hsiu, S.L., 2006, Pharmacokinetics and conjugation metabolism of naringin and naringenin in rats after single dose and multiple dose administrations, Journal of Food and Drug Analysis, 14(3), 247-253.

[9]Wang, N., Li, D., Lu, N.H., Yi, L., Huang, X.W. ve Gao, Z.H., 2010, Peroxynitrite and hemoglobinmediated nitrative/oxidative modification of human plasma protein: effects of some flavonoids, Journal of Asian Natural Products Research, 12(4), 257-64. https://doi.org/10.1080/10286021003620226.

[10]Wang, Y., Wang, S., Firempong, C.K., Zhang, H., Wang, M., Zhang, Y., Zhu, Y., Yu, J., Xu, X., 2017, Enhanced solubility and bioavailability o fnaringenin via liposomal nanoformulation: preparation and in vitro and in vivo evaluations, AAPS PharmSciTech, (2017) 18, 586–94. doi: 10.1208/s12249-016-0537-8.

[11]Wang, Z., Wang, S., Zhao, J., Yu, C., Hu, Y., Tu, Y., Yang, Z., Zheng, J., Wang, Y., Gao, Y., 2019, Naringenin ameliorates renovascular hypertensive renal damage by normalizing the

balance of reninangiotensin system components in rats, International Journal of Medical Sciences, 16, 644– 53. doi: 10.7150/ijms.31075.

[12]Wilcox, L.J., Borradaile, N.M. ve Huff, M.W., 1999, Antiatherogenic properties of naringenin, a citrus flavonoid, Cardiovascular Drug Reviews,17:160-178.

[13]Yao, L.H., Jiang, Y.M., Shi, J., Tomas-Barberan, F.A., Datta N., Singanusong, R., Chen, S. S., 2004, Flavonoids in food and their health benefits, Plant Foods for Human Nutrition, 59(3), 113-22. https://doi.org/10.1007/s11130-004- 0049-7.

[14]Alam, M.A., Subhan, N., Rahman, M.M., Uddin, S.J., Reza, H.M. ve Sarker, S.D., 2014, Effect of citrus flavonoids, naringin and naringenin on metabolic syndrome and their mechanisms of action, Advances, and Nutrition, 5(4), 404- 17. https://doi.org/10.3945/an.113.005603.

[15]Alberca, R.W., Teixeira, F.M.E., Beserra, D.R., de Oliveira, E.A., de Andrade, M.M.S., Pietrobon, A.J. ve Sato, M.N., 2020, Perspective: the potential effects of naringenin in COVID19, Frontiers in Immunology, (2020) 11, 1.

[16]Bourian, M., Runkel, M., Krisp, A., Tegtmeier, M., Freudenstein, J. ve Legrum, W., 1999, Naringenin and interindividual variability in interaction of coumarin with grapefruit juice, Experimental, and Toxicologic Pathology, (1999) 51, 289–93. doi: 10.1016/S0940-2993(99)80008-6.

[17]Breinholt, V.M., Svendsen, G.W., Dragsted, L.O. ve Hossaini, A., 2008, The citrus-derived flavonoid naringenin exerts uterotrophic effects in female mice at human relevant doses, Basic and Clinical Pharmacology and Toxicology, (2008) 94, 30–6. doi: 10.1111/ j.1742-7843.2004.pto_940106.x.

[18] Lee, H., Shao, H., Huang, Y. , Kwak, B., 2005. "Synthesis of MRI contrast agent by coating superparamagnetic iron oxide with chitosan," IEEE Transactions on Magnetics, vol. 41, no. 10, pp. 4102–4104

[19] Alhayali, N.I., Kalaycıoglu Ozpozan, N., Dayan, S., Ozdemir, N., Somtürk Yılmaz, B., 2021. Catalase/Fe_3O_4@Cu^{2+} hybrid biocatalytic nanoflowers fabrication and efficiency in the reduction of organic pollutants. Polyhedron,194,114888

[20]Somturk B, Hançer M, Öcsoy İ, Ozdemir N (2015). Synthesis of copper ion incorporated horseradish peroxidase based hybrid nanoflowers for enhanced catalytic activity and stability. Dalton Trans., 44(31):13845-13852. doi:10.1039/c5dt01250c

[21] Somturk B, Yilmaz I, Altinkaynak C, Karatepe A, Özdemir N, Ocsoy I (2016) Synthesis of urease hybrid nanoflowers and their enhanced catalytic properties. Enzyme Microb Technol 86:134–142. doi:10.1016/j.enzmictec.2015.09.005

[22] Ge, J., Lei, J.D., Zare, R.N. (2012), Protein-inorganic hybrid nanoflowers Nat. Nanotechnol., 7 , 428-432

[23]Noma, S.A., Somturk Yilmaz, B., Ulu, A., Ozdemir, N., Ateş, B. Development of l-asparaginase@hybrid Nanoflowers (ASNase@HNFs) Reactor System with Enhanced Enzymatic Reusability and Stability Catalysis Letters. 2021,151:1191-1201 DOI:10.1007/s10562-020-03362-1

[24] Somturk B, Dayan S, Ozdemir N, Kalaycıoğlu Özpozan N (2022), Catalytic performance improvement with metal ion changes for efficient, stable, and reusable superoxide dismutase–metalphosphates hybrid nanoflowers, Chem Pap 76:4245–4260. https://doi.org/10.1007/s11696-022-02179-z

[25] Celik, C., Ildiz, N., Ocsoy, I., 2020. Gallic acid nanoflower immobilized membrane with peroxidase-like activity for m-cresol detection Sci. Rep. https://doi.org/10. 1038/s41598-020-59699-5

[26] Koca, F.D., Matz Muhy, H., Halıcı, M.G., 2024. Catalytic and Antioxidant Activity of *Desmarestia menziesii* Algae Extract Based Organic@İnorganic Hybrid Nanoflowers. Journal of Inorganic and Organometallic Polymers and Materials, 34 (3), 1281-1292

[27] Koca, F.D., Matz Muhy, H., Halıcı, M.G., Gozcelioglu, B., Konuklugil, B., 2022. Synthesis of hybrid nanoflowers using extract of Ascoseira mirabilis, a large brown parenchymatous macroalga endemic to the Antarctic Ocean, as the organic component and evaluation of their antimicrobial, catalytic, and antioxidant activities. Applied Nanoscience (2023) 13:4787–4794 https://doi.org/10.1007/s13204-022-02618-z

[28] Maurya, S.S, Nadar, S.S., Rathod, V.K. 2020. Dual activity of laccaselysine hybrid organic–inorganic nanoflowers for dye decolourization. Environ Technol Innov 19:100798. https://doi.org/10.1016/j. eti.2020.100798

[29] Baldemir A, Köse NB, Ildiz N et al (2017) Synthesis and characterization of green tea (Camellia sinensis (L.) Kuntze) extract and its major components-based nanofowers: a new strategy to enhance antimicrobial activity. RSC Adv 7:44303–44308. https://doi.org/ 10.1039/c7ra07618e

[30] Agarwal M, Bhadwal AS, Kumar N, Shrivastav A, Shrivastav BR, Singh MP, Zafar F, Tripathi RM (2016) Catalytic degradation of methylene blue by biosynthesised copper nanoflowers using F. benghalensis leaf extract. IET Nanobiotechnol 10:321–325. https://doi.org/10.1049/iet-nbt.2015.0098

[31] Demirbas A (2021) Comparison study of synthesized red (or blood) orange peels and juice extract-nanoflowers and their antimicrobial properties on fsh pathogen (Yersinia ruckeri). Indian J Microbiol 61:324–330. https://doi.org/10.1007/s12088-021-00945-3

[32] Gan J, Ashraf SS, Bilal M, Iqbal HM (2022) Biodegradation of environmental pollutants using catalase-based biocatalytic systems. Environ Res 214:113914. https://doi.org/10.1016/j.envres.2022. 113914

[33] Geltmeier, A., Rinner, B., Bade, D., Meditz, K., Witt, R., Bicker, U., Bludszuweit-Philipp, C., Maier, P., 2015.Characterization of Dynamic Behaviour of MCF7 and MCF10A Cells in Ultrasonic Field Using Modal and Harmonic Analyses. PLoS One. 2015; 10(8): e0134999.

[34] Somturk Yilmaz, B., 2024. Antimicrobial and Anticancer Activity of Gallic Acid–Cu(II) Hybrid Nanofowers and Gallic Acid–Zn(II) Hybrid Nanofowers. Journal of Inorganic and Organometallic Polymers and Materials https://doi.org/10.1007/s10904-024-03169-2

[35] Bor, E., Koca Caliskan, U., Anlas, C., Durbilmez, G.D., Bakirel, T., Ozdemir, N., 2022. Synthesis of *Persea americana* extract based hybrid nanoflowers as a new strategy to enhance hyaluronidase and gelatinase inhibitory activity and the evaluation of their toxicity potential, Inorg. Nano-Met.1–3, https://doi.org/10.1080/ 24701556.2022.2072342.